# PHASE COMPOSITION STABILITY OF ZrN/SiN$_x$ MULTILAYERED COATINGS UNDER AIR ANNEALING: THE ROLE OF THE THICKNESSES RATIO OF THE ELEMENTARY LAYERS

I.A. Saladukhin[1)], G. Abadias[2)], S.V. Zlotski[1)], A.A. Malashevich[1)]

[1)]*Belarusian State University, 4 Nezavisimosti Ave., 220030 Minsk, Belarus, solodukhin@bsu.by*

[2)]*Institut P', Université de Poitiers-CNRS-ENSMA, SP2MI, Téléport 2, F86962 Chasseneuil-Futuroscope, France, gregory.abadias@univ-poitiers.fr*

In the present work the phase composition stability and oxidation resistance of ~300 nm thick ZrN/SiN$_x$ nanoscale multilayers at the air annealing procedure were studied. Coatings were prepared by reactive magnetron sputter-deposition on Si wafers under Ar+N$_2$ plasma discharges. ZrN/SiN$_x$ multilayers with ZrN and SiN$_x$ layer thickness varying from 2 to 10 nm were synthesized by sequential sputtering from elemental Zr and Si$_3$N$_4$ targets at $T_{dep}$ =300 °C. According to X-ray diffraction (XRD) analysis the multilayered films consist of nanocrystalline (002)-oriented ZrN and amorphous SiN$_x$ layers. The oxidation resistance under air was studied using in situ XRD in the temperature range from 400 to 950 °C, as well as by scanning electron microscopy (SEM) and wavelength dispersive X-ray spectrometry (WDS) after air annealing procedure. While the reference ZrN film starts to oxidize at $T_{ox.}$ = 550 °C, a much higher oxidation resistance is found for multilayered films, till $T_{ox.}$ = 860–950 °C for ZrN/SiN$_x$ coatings with the elementary layer thickness ratio of 5 nm/10 nm and 2 nm/5 nm.

***Keywords***: zirconium nitride; silicon nitride; phase composition; oxidation resistance.

## Introduction

Thin films on the basis of nitrides of transitional metals (TM) are widely used as hard protective coatings in the industry. These coatings are characterized by high wear resistance, high adhesion, hardness and oxidation resistance, which are related to a combination of their structure and phase composition stability. For this purpose, the coatings on the basis of mononitrides (TiN, CrN, ZrN, etc.) are applied as well as the multicomponent systems [1]. One of the most important properties of the coatings for their practical application is their resistance to high temperature oxidation. For this purpose, most of the mononitride films cease to perform their protective function. For example, TiN coatings are rapidly oxidized at temperatures as low as 550 °C [2].

One of the promising options for both improvement of mechanical characteristics and increase in a resistance to high-temperature oxidation is the formation of multilayered film structures. Multilayers consisting of alternate stacking of TM nitride and SiN$_x$ layers are characterized by limited intermixing, due to the strong immiscibility between these two phases [3,4], which makes them perspective candidates for the achievement of high thermal stability. In addition, the presence of numerous interfaces between the layers suppresses the formation of columnar structure of a coating [3] that, in turn, interferes with the formation of the continuous pores. The abovementioned factors enable to consider such multilayers as potential materials for applications under high-temperature corrosion conditions.

The present work aims at contributing to the role of the thicknesse ratio of the elementary layers onto the phase composition stability and oxidation resistance of ZrN/SiN$_x$ multilayered coatings.

## Experimental details

Multilayered ZrN/SiN$_x$ films were grown by reactive magnetron sputter-deposition in a high vacuum chamber (base pressure < $10^{-5}$ Pa) equipped with three confocal targets configuration and a cryogenic pump (max. 500 l/s). Films were deposited on Si substrates at 300 °C. A constant bias voltage of −60 V was applied to the substrate during deposition. ZrN/SiN$_x$ multilayers with ZrN and SiN$_x$ layer thickness varying from 2 to 10 nm were synthesized. Monolithic ZrN and SiN$_x$ films were also deposited as the reference films. The total film thickness was ~300 nm.

Water-cooled, 7.62-cm-diameter Zr (99.92% purity), Si (99.995% purity, p-type doped) and Si$_3$N$_4$ (99.99% purity) targets, located at 18 cm from the substrate holder, were used under Ar+N$_2$ plasma discharges at constant power mode. The Zr and Si target were operated in magnetically unbalanced configuration using a DC power supply, while a RF power supply was used for the Si$_3$N$_4$ target in balanced mode. The total working pressure was 0.21 Pa.

X-ray Diffraction (XRD) analysis was employed for structural identification using a D8 Bruker AXS X-ray diffractometer operating in Bragg–Brentano configuration and equipped with CuK$_\alpha$ wavelength (0.15418 nm) and LynxEye detector.

The films were annealed at ambient air at different sequential temperatures from 400 °C up to 950 °C. The oxidation process was investigated using in situ XRD experiments. The samples were placed on a resistive heating stage implemented on the Bruker D8 diffractometer, consisting in an AlN sample holder and a hemispheric graphite dome. Total scan time during isothermal annealing was 40–60 min.

The elemental composition of films in their as-deposited and air-annealed states was determined using elemental probe microanalysis. A wavelength dispersive spectrometer (WDS) unit from Oxford Instruments attached to a JEOL 7001 TTLS scanning electron microscope (SEM) operated at 10 kV and 10 nA was used for the quantification with a precision better than 1 at.%. The same microscope was used for obtaining top-view SEM micrographs of the films after air annealing at 950 °C.

## Results and discussion

As described in the previous section, the ZrN/SiN$_x$

films were formed with different ZrN to $SiN_x$ layer thickness ratios, that is, with various fractions of ZrN layer, $f_{ZrN}$. The elemental composition of the individual layers in multilayered systems corresponds to composition of ZrN and $SiN_x$ monolithic reference films: 46.6 at.% Zr and 53.4 at.% N for ZrN film, 43.3 at.% Si and 56.7 at.% N for $SiN_x$ film.

The angular region of XRD patterns covering the main 111 and 200 Bragg reflections for ZrN monolithic reference and $ZrN/SiN_x$ multilayered films is shown in Fig. 1-2 (see lower curves for as-deposited state). The main features of $ZrN/SiN_x$ multilayered structures formation are the following: 1) there is a change in preferred orientation from (111) that is inherent to ZrN film to (200) due to repeated nucleation of ZrN layers on amorphous $SiN_x$ layers; 2) the broadening of 200 ZrN peak with decreasing $f_{ZrN}$ occurs (that corresponds to crystallite size decrease) together with a shift to lower 2θ values (that indicates increase in the lattice parameter of ZrN phase due to growth of compressive stress); 3) both $SiN_x$ monolithic reference film and $ZrN/SiN_x$ multilayered films with ZrN layer thickness 2 nm are XRD amorphous. The tendency of transition to (200) preferred orientation and subsequent broadening of 200 ZrN peak with decreasing $f_{ZrN}$ for $ZrN/Si_3N_4$ nanomultilayers was also observed by Dong et al. [5]. Therefore, the insertion of amorphous a-$SiN_x$ layers influences on the structure of growing ZrN layers.

The evolution of XRD patterns for ZrN monolithic reference film and $ZrN/SiN_x$ multilayered films during in-situ air annealing is also presented in Fig. 1-2. For ZrN film, the formation of tetragonal t-$ZrO_2$ oxide is already registered at the temperature of 550 °C (Fig. 1). Above this temperature, that is after annealing at $T_{ann.}$ = 700 °C, the Bragg reflections from the cubic ZrN phase are no longer visible. At $T_{ann.}$ = 950 °C the monoclinic (m-$ZrO_2$), which is the stable form of zirconia below 1170 °C, and tetragonal (t-$ZrO_2$) zirconium oxides are revealed in the film composition. It should be mentioned that no crystalline oxide phases could be detected for the air-annealed $SiN_x$ reference film.

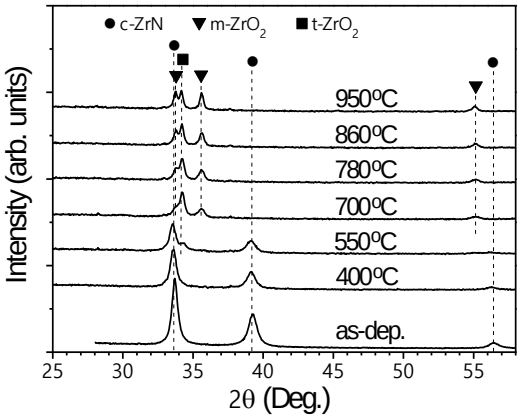


Fig. 1. Evolution of XRD patterns under air annealing for ZrN reference film

In Fig. 2, XRD patterns for $ZrN/SiN_x$ multilayered films are shown in the sequence of reduction of ZrN layer fraction, $f_{ZrN}$. For $ZrN/SiN_x$ (5 nm/2 nm) and $ZrN/SiN_x$ (10 nm/5 nm) film the crystallization of t-$ZrO_2$ phase occurs at 700–780 °C (Fig. 2a-b), while for the $ZrN/SiN_x$ (10 nm/10 nm) and $ZrN/SiN_x$ (5 nm/5 nm) films it takes place at 860 °C (Fig. 2c-d). If we compare now the results between $ZrN/SiN_x$ films with close ratio of ZrN layer thickness to $SiN_x$ layer thickness, namely (5 nm/2 nm) and (10 nm/5 nm) as well as (10 nm/10 nm) and (5 nm/5 nm), one can see that when the bi-layer period is reduced, the resistance to oxidation is further improved (Fig. 2a and 2d).

For $ZrN/SiN_x$ (5 nm/5 nm) film (Fig. 2d) as well as for $ZrN/SiN_x$ (5 nm/10 nm) and $ZrN/SiN_x$ (2 nm/5 nm) films (Fig. 2e and 2f), no trace of m-$ZrO_2$ is detected during annealing. In the case of $ZrN/SiN_x$ (5 nm/10 nm) film (Fig. 2e), the ZrN peak remains till the temperature of 950 °C inclusive. Therefore, the analysis of in-situ temperature XRD patterns of $ZrN/SiN_x$ multilayered films confirms that the resistance to oxidation is significantly improved when either decreasing of fraction of ZrN layer, $f_{ZrN}$, and/or increasing the interfaces density (quantity of layers in the film).

The fact that the $ZrN/SiN_x$ (2 nm/5 nm) film, which is X-ray amorphous in the as-deposited state, remains fully amorphous after annealing, with no crystalline oxide phases being detected up to 950 °C (Fig. 2f), is also interesting for application purposes. This result is in line with the excellent high-temperature oxidation resistance generally observed for nitride-based amorphous alloys [6].

Study of the surface morphology of $ZrN/SiN_x$ films by SEM method, as well as their elemental composition by WDS method, after annealing in air at the temperature of 950 °C confirms the results of XRD analysis. Firstly, the coating resistance to oxidation increases when $f_{ZrN}$ decreases. It means that $ZrN/SiN_x$ films, for which the thickness of ZrN elementary layer is less than the thickness of $SiN_x$ elementary layer, possess the greater stability. Secondly, the oxidation resistance becomes higher at the increase in quantity of layers in the film (at the same total film thickness). The last factor can be caused by both the increase in number of interfaces between layers that impede the oxygen diffusion deep into the film and by the modification of zirconium nitride structure which consists in the decrease of crystallite size when reducing the thickness of ZrN elementary layer.

Elemental analysis data for $ZrN/SiN_x$ (5 nm/2 nm), $ZrN/SiN_x$ (10 nm/5 nm), $ZrN/SiN_x$ (10 nm/10 nm) and $ZrN/SiN_x$ (5 nm/5 nm) films after air annealing testify its almost complete oxidation as well as in the case of ZrN monolithic reference film. Such behavior is typical for multilayered films with the high fraction of ZrN layer, $f_{ZrN}$. Meanwhile, $ZrN/SiN_x$ (5 nm/10 nm) film is rather stable under air annealing. There are only isolate small corrosion sites. Anyway, the oxygen content in this film is significantly less than for the films with the high $f_{ZrN}$. In the case of $ZrN/SiN_x$ (2 nm/5 nm) film, the corrosion sites which lead to its swelling are not registered. According to elemental analysis, the superior stability is characteristic for this film under high-temperature annealing in air.

Thus, the analysis of $ZrN/SiN_x$ multilayered films by XRD, SEM and WDS methods enables to make a conclusion on their higher resistance to oxidation at the elevated temperatures in comparison with ZrN and $SiN_x$ films. The absence of microcracks and pores in the oxidized coatings slows down the inward oxygen diffusion and hence improve the oxidation resistance compared to monolithic reference coatings.

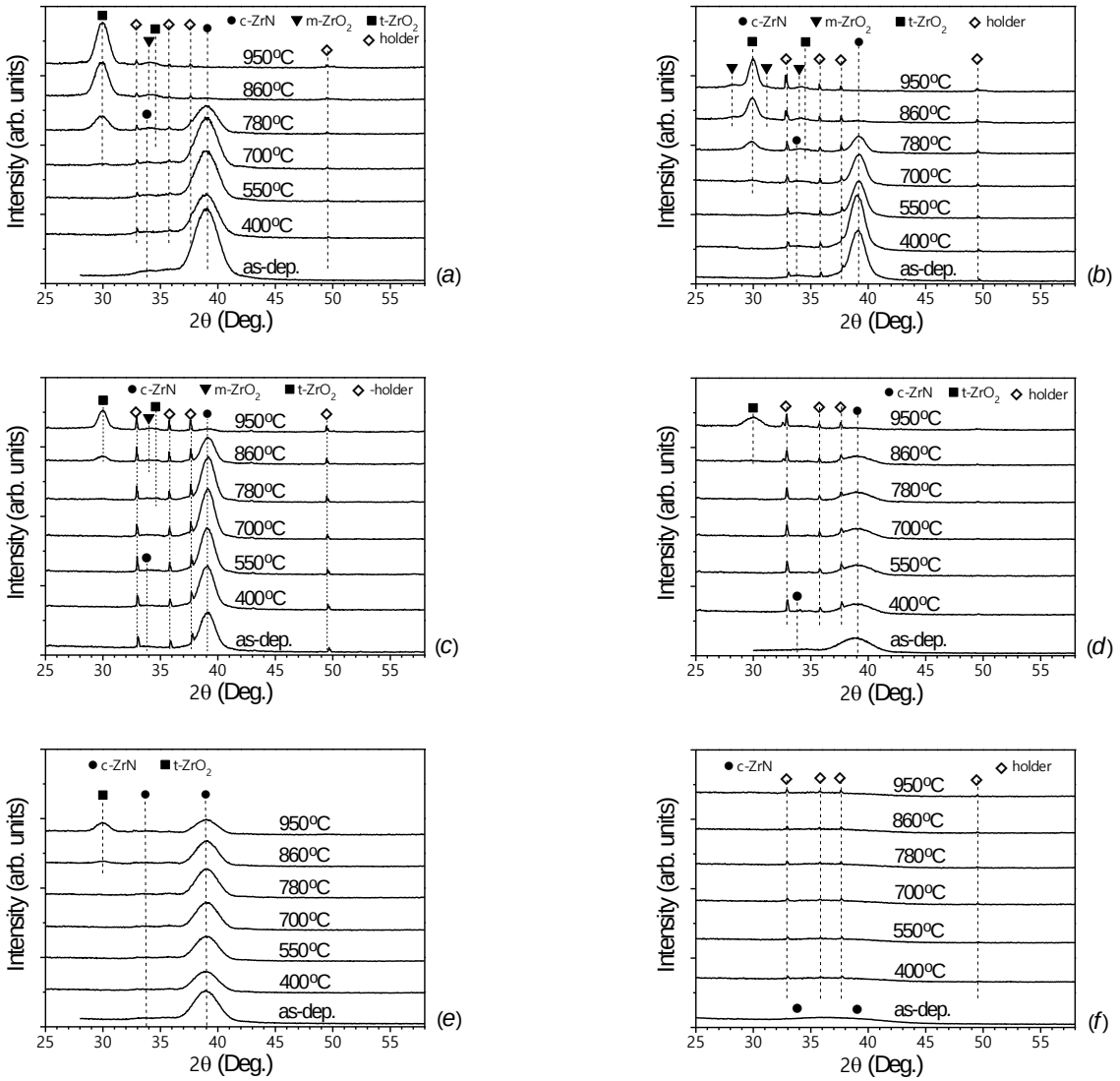


Fig. 2. Evolution of XRD patterns under air annealing for $ZrN/SiN_x$ multilayered films with different thickness ratio of ZrN and $SiN_x$ elementary layers: *a* – 5 nm/2 nm, *b* – 10 nm/5 nm, *c* – 10 nm/10 nm, *d* – 5 nm/5 nm, *e* – 5 nm/10 nm and *f* – 2 nm/5 nm.

## Conclusions

Nanoscale $ZrN/SiN_x$ multilayered films with various thickness ratio of elementary layers were synthesized by magnetron sputter deposition method. Films consist of highly periodic nanocrystalline (002)-oriented ZrN and amorphous $SiN_x$ layers. Reducing the ZrN layer thickness fraction with respect to bilayer thickness, $f_{ZrN}$, leads to decrease in crystallite size and increase in the lattice parameter of ZrN phase due to larger compressive stress.

$ZrN/SiN_x$ multilayered films are characterized by higher resistance to oxidation at the temperatures up to 950 °C in comparison with ZrN and $SiN_x$ monolithic reference films. Oxidation resistance of $ZrN/SiN_x$ films increases when reducing $f_{ZrN}$ as well as increasing interface density. $ZrN/SiN_x$ films with ZrN to $SiN_x$ thicknesses ratio of 5 nm/10 nm and 2 nm/5 nm are considered to be the best candidates for use at the elevated temperatures.

## References

1. Aninat R., Valle N., Duday D., Choquet P. Structural properties and high temperature oxidation behaviour of Al-Ti-Ta-N and Al-Ti-Ta-Y-N coatings. *Corros. Sci.* 2016; 111: 454-466.
2. Abadias G., Koutsokeras L.E., Siozios A., Patsalas P. Stress, phase stability and oxidation resistance of ternary Ti–Me–N (Me = Zr, Ta) hard coatings. *Thin Solid Films* 2013; 538: 56-70.
3. Soares T.P., Aguzzoli C., Soares G.V., Figueroa C.A., Baumvol I.J.R. Physicochemical and mechanical properties of crystalline/amorphous $CrN/Si_3N_4$ multilayers. *Surf. Coat. Technol.* 2013; 237: 170-175.
4. Abadias G., Uglov V.V., Saladukhin I.A., Zlotski S.V., Tolmachova G., Dub S.N. et al. Growth, structural and mechanical properties of magnetron-sputtered $ZrN/SiN_x$ nanolaminated coatings. *Surf. Coat. Technol.* 2016; 308: 158-167.
5. Dong Y., Zhao W., Yue J., Li G. Crystallization of $Si_3N_4$ layers and its influences on the microstructure and mechanical properties of $ZrN/Si_3N_4$ nanomultilayers. *Appl. Phys. Lett.* 2006; 89: 121916 (1-3).
6. Musil J. Hard nanocomposite coatings: thermal stability, oxidation resistance and toughness. *Surf. Coat. Technol.* 2012; 207: 50-67.